



OPEN ACCESS

EDITED BY

Sen Wang,
China University of Petroleum
(East China), China

REVIEWED BY

Wenxue Han,
Shandong University of Science and
Technology, China
Weijiao Ma,
China University of Petroleum
(East China), China

*CORRESPONDENCE

Senhu Lin,
✉ lsh2012@petrochina.com.cn
Xia Luo,
✉ luoxia69@petrochina.com.cn
Zhongying Zhao,
✉ zhaozhongying@petrochina.com.cn

RECEIVED 28 October 2024

ACCEPTED 23 December 2024

PUBLISHED 22 January 2025

CITATION

Lin S, Luo X, Zhao Z, Hou L, Li S, Li H, Pang Z
and Zhang L (2025) Grading evaluation
methods for lacustrine shale oil resources
developed by *in-situ* heating conversion
technology.
Front. Earth Sci. 12:1518236.
doi: 10.3389/feart.2024.1518236

COPYRIGHT

© 2025 Lin, Luo, Zhao, Hou, Li, Li, Pang and
Zhang. This is an open-access article
distributed under the terms of the [Creative
Commons Attribution License \(CC BY\)](#). The
use, distribution or reproduction in other
forums is permitted, provided the original
author(s) and the copyright owner(s) are
credited and that the original publication in
this journal is cited, in accordance with
accepted academic practice. No use,
distribution or reproduction is permitted
which does not comply with these terms.

Grading evaluation methods for lacustrine shale oil resources developed by *in-situ* heating conversion technology

Senhu Lin^{1*}, Xia Luo^{1*}, Zhongying Zhao^{1*}, Lianhua Hou¹,
Shixiang Li², Hui Li³, Zhenglian Pang¹ and Lijun Zhang¹

¹Research Institute of Petroleum Exploration and Development, PetroChina, Beijing, China, ²CNPC Shenzhen New Energy Research Institute Co., Ltd., Shenzhen, China, ³School of Information and Communications Engineering, Xi'an Jiaotong University, Xi'an, China

In-situ conversion technology is a sustainable and effective method of recovering medium-low maturity shale, which can be produced with oil resources expected to exceed global total proven oil reserves. Nevertheless, criteria and procedures for grading such shale oil resources are lacking. We present a combination of distinct facies and theoretical economic index (I_e) to grade the *in-situ* conversion shale oil resources of Chang 7 Member in the Ordos Basin and Nenjiang Formation in the Songliao Basin. This shale oil resource was categorized into four classes: invalid, valid, sweet-spot and core resource. For the shale dominated by type II kerogen (Chang 7), total organic carbon (TOC) values at 6%, 9%, and 12%, hydrocarbon generation potential (S_1+S_2) values at 15 mg/g, 30 mg/g, and 50 mg/g, and I_e at 2, 3, and 4, respectively, represent the boundary of the four resource grades. For the shale dominated by type I kerogen (Nenjiang), TOC values at 4%, 6%, and 8%, S_1+S_2 values at 19 mg/g, 32 mg/g, 48 mg/g, and I_e at 2, 3, and 4, respectively, represent the boundary of the four resource grades. Our research provides a feasible practical strategy for evaluating and predicting *in-situ* conversion shale oil resources in lacustrine basins.

KEYWORDS

shale oil, *in-situ* conversion, resource grading, theoretical economic index, the Ordos Basin

1 Introduction

Shale in medium-low maturity contains kerogen and some retained hydrocarbons. Kerogen cannot be exploited using current fracturing technique and liquid hydrocarbons cannot be extracted economically because of the poor reservoir drive. As a result, it is challenging to exploit medium-low maturity shale oil resources at present. By placing heaters in the target formation, *in-situ* shale oil conversion is achieved through heating the shale, which facilitates thermal cracking, heavy oil upgrading, desulfurization, and hydrogenation. This process converts kerogen and heavy hydrocarbons into hydrogen, hydrogen sulfide, natural gas, liquefied petroleum gas (LPG), and light oil—comprising primarily fractions such as gasoline, aviation kerosene, and diesel. Furthermore, the products are extracted

to the surface via wells (Sun et al., 2023). The benefits of this technology are modest surface area coverage, low cost, negligible environmental impact, and viability for deep shale oil resource exploitation (Sun et al., 2023).

Incomplete estimates place the global medium-low maturity shale oil resources at 689 billion tons (Kang et al., 2020). The United States has the world's largest medium-low maturity shale oil resources, accounting for about 77% of potentially recoverable shale oil (Dyni, 2003). China's medium-low maturity shale oil resources are estimated as 47.6 billion tons (Liu et al., 2017), ranking second in the globe (Liu et al., 2006). Based on most recent experimental simulation data, the estimated total shale oil reserves developed by *in-situ* heating conversion technology are 49.4 billion tons for the Chang 7 Member in the Ordos Basin and 37.7 billion tons for the Nenjiang Formation in the Songliao Basin (Zhao et al., 2023a). These two fields, which represent type II and type I kerogen lacustrine shales in China, have significant potential for *in-situ* conversion shale oil exploitation.

In comparison, the global risk geological reserves of shale oil of medium-high maturity are about 248.8 billion tons, and the risk recoverable reserves are about 13 billion tons (EIA, 2013). Estimates of China's medium-high maturity shale oil resources vary widely. U.S. Energy Information Administration (EIA) estimated 4.5 billion tons of technically recoverable medium-high maturity shale oil in China (EIA, 2013). Sinopec estimated 7.4 to 37.2 billion tons of technically recoverable medium-high maturity shale oil in the major lacustrine basins in China (Jin et al., 2019). PetroChina estimated that China has 10 billion tons of medium-high maturity shale oil in place. According to the statistical results, shale oil resources in medium-low maturity are approximately three times larger than those in medium-high maturity (Zhao et al., 2020).

Shell, ExxonMobil, Total, and other major oil firms have committed to conducting *in-situ* conversion technology research and field tests (Wang et al., 2013). Shell's *In-situ* Conversion Process (ICP) technology is now the most advanced, having completed many field testing in the United States and Jordan that are ready for industrial deployment (Alpak et al., 2013). However, the utilization of *in-situ* conversion shale oil remains in its early stages. One reason is the high price. If technological and economic constraints can be overcome, this field will have a significant influence on global fossil energy supply patterns.

Research on the resource grading of *in-situ* conversion shale oil is still scarce. A preliminary resource assessment of China was conducted by certain experts, who also proposed a lower limit for *in-situ* conversion shale oil (Hu et al., 2020; Zhao et al., 2018). Guo et al. (2022) specified the core and sweet-spot area but did not define them or explain the division principles. It also provided a set of evaluation methodologies for *in-situ* conversion shale oil resource and evaluated the total quantity of *in-situ* conversion shale oil resources in the Ordos Basin, China. Guo et al. (2023) used the hydrocarbon generation quantity approach based on hydrogen index fluctuation to compute the resource amount of *in-situ* conversion shale oil in China, which is up to 46.03 billion tons. They did not, however, create evaluation standards for resource grading (Guo et al., 2023).

The objective of this study is to provide a feasible standard for the grading evaluation of *in-situ* conversion shale oil resource, so

as to guide the exploration and development of this resource. *In-situ* conversion of shale oil involves a large amount of heat input, so resource grading should consider the hydrocarbon generation potential and the economics of development. Hydrocarbon generation potential is the material basis and the premise of *in-situ* conversion shale oil. It is regarded as the first factor of resource grading evaluation. The economics of development is related to technology, investment, oil price (Cui et al., 2018), etc., and multiple variables exist in different situations, making it difficult to analyze using a single criterion. The theoretical economics of the *in-situ* conversion of shale oil was investigated through the utilization of the calorific value of the hydrocarbons generated by *in-situ* conversion and the energy needed to achieve kerogen conversion. Findings and interpretations from this research contribute to longer range efforts being made to: 1) understanding the role of facies in *in-situ* conversion shale oil resource abundance; 2) recognize implications of thermal evolution and organic matter types in shale reservoirs; 3) Grade shale oil resources according to various development modes in terms of energy and value substitution.

2 Method details

2.1 Samples and experimental data

This study uses core data to: 1) identify facies and 2) give an in-depth analysis of organic geochemical characteristics. 806 core samples were taken from 72 wells in the Southern Ordos Basin. Additionally, 201 core samples' geochemical data were gathered from 11 wells in the Songliao Basin. The following analytical data were used in this study: 6 activation energy analysis samples, 1,007 source rock analysis samples, 992 TOC core-based measurements, and 6 sets of thermal simulation experiment findings. The shale samples of this study are all in the low-to-medium maturity stage.

TOC analyses and source rock pyrolysis were provided for the 72 wells in this study. The TOC was measured on the LECOCS230 instrument. The free hydrocarbons (S_1) and pyrolyzed hydrocarbons (S_2) was measured on the Rock-Eval 6 pyrolyzer by VINCI, France. Activation energy analysis was carried out on shale samples from 6 wells. The experiment was performed using the activation energy analysis module of Rock-Eval II pyrolyzer in the State Key Laboratory of Petroleum Resources and Exploration, China University of Petroleum (Beijing). The calculation of hydrocarbon generation kinetics is based on the method of chemical reaction velocity and Arrhenius' empirical formula (Arrhenius, 1889). In terms of the time-temperature compensation relationship (Connan, 1974), based on the laboratory data of high temperature and rapid shale cracking simulation, with American Lawrence Livermore national LABS KINETICS 2015-Code Version 6.110 dynamics software version, we used parallel first order kinetics reaction model to calculate the activation energy.

2.2 Isoline maps

In this study, TOC isoline map (Guo et al., 2020), vitrinite reflectance (R_o) isogram (Zhao et al., 2018), shale isopach map (Lin et al., 2019) and hydrocarbon generation potential (S_1+S_2)

isoline map (Guo et al., 2022) of Chang 7 shale in the Ordos Basin were collected from published literatures. The TOC and S_1+S_2 isoline maps were partially corrected according to our experimental results data.

2.3 Classification method of facies

Facies are rocks or combinations of rocks formed in a certain sedimentary environment. In this study, a facies represents the shale samples that are mainly similar in geological and geochemical characteristics and may originate analogously (Lin et al., 2019). Geostatistical decision tree method is used to classify shale facies. The method consists of the following main steps: 1) Build a geostatistical decision tree based on the experimental results (training data) of some samples. 2) Rapidly evaluated genetic relationships among these shale samples with hierarchical cluster analyses. 3) Identify several distinct shale facies according to the cluster distance of the clustering result. 4) Based on the cause-related data, apply the multitiered decision tree to classify additional shale samples those may be data incomplete (only partial experimental analysis has been completed). 5) Calculate the confidence coefficient.

With respect to training data, it is beneficial to have more parameters in more samples. The principles of parameter selection include: 1) It should have a clear indication meaning; 2) It should be generally considered to represent the main characteristics; 3) It should have sensitive response and no multi-solution. In this study, a geostatistical decision tree with 22 parameters established by Lin et al. (2019) for Chang 7 shale in the Ordos Basin is used. These parameters enable us to differentiate the samples, including sedimentology, rock geochemistry, fluid geochemistry and organic petrology, on behalf of the most significant visual characteristics, formation environment, OM types, and content and type of recoverable hydrocarbon.

2.4 Calculation method of theoretical economic index

Compared to medium-high maturity shale oil, *in-situ* conversion shale oil is easier to exploit, with a recovery rate of up to 70% (Zhao et al., 2018). The key constraint on the development of *in-situ* conversion shale oil is economic viability, which includes three major factors (Yu et al., 2023). The first factor is the investment cost, including drilling, surface engineering, oil recovery engineering, and heating equipment costs. Operating costs can be considered to be the second factor, and they include energy consumption for heating such as electricity costs. The last factor is oil prices. The parameters for economic evaluation are uncertain due to a number of factors, including the differences in the development level of various shale oil areas, variations in energy consumption due to different development methods, and fluctuations in oil prices. As a result, in this study, we started from the mechanism of *in-situ* conversion, and we only considered the required thermal energy for completing the conversion of the organic matter as the input and the total heat of hydrocarbon production as the output. The ratio of

the input to the output of these two energies was used to evaluate the theoretical economic viability of *in-situ* conversion shale oil.

$$I_e = Q * r / E \quad (1)$$

$$Q = m_1 * q_1 + m_2 * q_2 + \dots + m_i * q_i \quad (2)$$

$$E = E_{rock} + E_{kero} \quad (3)$$

where I_e is the theoretical economic index; Q is the total heat content released by complete combustion of the *in-situ* conversion hydrocarbon products (J); r is the recovery rate of *in-situ* converted shale oil; m_i is the mass of component i produced per unit mass of shale (kg); q_i is the heat value of component i (J/kg); E is the total input thermal energy for the *in-situ* conversion of shale per unit mass (J); E_{rock} is the total input thermal energy for heating one unit mass of rock to a specified temperature (J); and E_{kero} is the total input thermal energy for the complete conversion of one unit mass of kerogen (J).

In Equation 1, r is determined by the basin geology and the specific development process. In Equation 2, the yields of the various components are determined via thermal simulation experiment. In Equation 3, the specified temperature is determined by the activation energy of kerogen (Zhang et al., 1983; Deng et al., 2020). I_e is equal to 1, indicating that the heat of the extracted hydrocarbon is equal to the input thermal energy. This suggests that a higher I_e value indicates better economic viability. All of the above quantitative values, the temperature of the complete conversion, and the recovery rate are used for economic evaluation and are derived from the latest thermal simulation experiments conducted by the *In-situ* Conversion Laboratory of the Research Institute of Petroleum Exploration and Development.

3 Results and discussion

3.1 Boundary values of resource grading parameters according to facies heterogeneity

Many parameters can be used for resource evaluation of shale oil developed by *in-situ* heating conversion technology, such as TOC, chloroform bitumen "A," porosity, oil saturation, etc. The pyrolysis hydrocarbon generation potential (S_1+S_2) can be considered as a geochemical indicator that directly reflects the *in-situ* conversion shale oil yield; however, due to differences in the cause of the formations, different shale facies have significantly different kerogen types, total organic carbon (TOC) contents, and hydrocarbon generation potentials. Therefore, in this study, the facies, TOC, and S_1+S_2 are combined to establish a quick grading evaluation standard for *in-situ* conversion shale oil by using as few parameters as possible.

According to the experimental findings, there are three facies that may be distinguished in the Chang 7 Member shale (Lin et al., 2019). Facies A_y shale has extremely rich organic laminae, with laminae spacing typically ranging from 0.1 to 1 mm (Figure 1A). The majority of this shale facies may have been deposited in deep water. Facies B_y shale has an organic lamina density that is roughly three

to five times higher than that of facies C_y shale. It is frequently semi-continuous or fuzzy, with a lamina spacing of between 0.5 and 2 mm (Figure 1B). Its structure is deformed in ways including bending, rolling, and folding. This shale facies may be formed in semi-deep lakes and is subject to frequent gravity flow. Facies C_y shale has highly flat, but uncommon, organic laminae with a large laminae spacing of typically 1–10 mm (Figure 1C). With inadequate particle sorting, the sediment between the organic laminae is primarily composed of silt and mud (Figure 1C). The density of organic lamina indicates that the organic carbon abundance of facies C_y shale is the lowest, and that of facies A_y shale is the largest. Furthermore, entire algal remains—which could be diatom shells with a great resistance to degradation—are frequently retained in facies A_y shales.

The three shale facies have average TOC contents of 14.6%, 3.8%, and 1.3%, respectively (Table 1). The maximum TOC, free hydrocarbon (average S_1 of 4.82 mg/g), and pyrolysis hydrocarbon (average S_2 of 59.11 mg/g) levels are found in the facies A_y shale. Type II_1 kerogen, which has a relatively high potential for hydrocarbon generation, predominates in the facies A_y shale. The type II_2 kerogen predominates in the facies B_y shale, and all of its geochemical parameter values—aside from the hydrogen index—are lower than those of the facies A_y shale. Furthermore, type III kerogen predominates in the facies C_y shale, which has the lowest geochemical parameter values (Table 1).

The shale of the Nenjiang Formation in the Songliao Basin was also divided into three facies. The maximum TOC content (8.1%) and S_1+S_2 value (53.21 mg/g) were identified in the facies A_n shale, whereas the medium TOC content (5.5%) and S_1+S_2 value (30.59 mg/g) were found in the facies B_n shale. With a TOC content of 3.0% and an S_1+S_2 value of 16.57 mg/g, the facies C_n shale has the lowest values. Furthermore, the hydrogen index of shales from three facies show a sequential decrease, but remain above 500 mg/g, indicating that Type I kerogen predominates in the Nenjiang Formation shale.

Due to facies heterogeneity, the relationship between $S_1 + S_2$ and TOC exhibits distinct zonal features (Figure 2A). Thus, the resource grading boundary can be tentatively determined as the border of the (S_1+S_2) zones. This approach has a theoretical foundation in addition to being simple to use in real-world situations. As can be seen, the facies C_y shale mainly has TOC values of <6.2% and S_1+S_2 values of <15 mg/g; the facies B_y shale mainly has TOC values of <9.1% and S_1+S_2 values of <30 mg/g; and the facies A_y shale mainly has TOC values of >9.1% and S_1+S_2 values of >30 mg/g. Therefore, the relationship between the TOC and S_1+S_2 reflects the facies heterogeneity. At the border between facies C_y and B_y , the TOC is 6.2% and S_1+S_2 is 15 mg/g (Table 2); at the border between facies B_y and A_y , the TOC is 9.1% and S_1+S_2 is 30 mg/g (Table 2). Similar different zonal features are shown in the connection between S_1+S_2 and TOC of shales in the Nenjiang Formation (Figure 2B). They both had TOC boundary values that were less than that of the Chang 7 shale, at 3.7% and 6.0%, respectively (Table 2). The values of their S_1+S_2 boundary were 19 mg/g and 32 mg/g, respectively, which were higher than the values of Chang 7 shale. (Table 2). The variations in kerogen types between the two sets of shale formations need to be connected to this feature.

The facies B_y shale has a medium potential to convert *in-situ* shale oil resources, so it can be classified as containing valid resources for future exploration and development. It is suggested that the facies C_y

shale was classified as containing invalid resources because it has a relatively poor hydrocarbon generation potential and its resources are difficult to develop economically. Since the facies A_y shale has the greatest potential to produce hydrocarbons, it can be categorized as having sweet-spot resources for appraisal and development in the near future. Additionally, at the S_1+S_2 value of 50 mg/g, the trend line of scatter plot of facies A_y (Figure 1A) intersects the upper limit of S_1+S_2 of facies B_y shale, and the associated TOC is equal to 12.1%. Based on this, we determined that the shales with TOC >12.1% and S_1+S_2 > 50 mg/g contain the core resource, which merits priority exploration and development (Table 2). Likewise, the facies A_n shale in Nenjiang Formation is further divided into two sub-regions, and within those, shales possessing core resources are defined as having TOC >8.2% and S_1+S_2 > 48 mg/g (Table 2).

3.2 Maturity constraints

Thermal maturity of the organic matter places a major constraint on the abundance of *in-situ* conversion shale oil resources. Even though a high maturity shale is rich in organic matter, it could not have a good potential to yield hydrocarbons (Pang and Chen, 1997). Thermal maturity should thus be one of the parameters used to properly identify the grading of *in-situ* conversion shale oil.

When it comes to *in-situ* conversion of shale oil, type III kerogen—even in extremely high abundance—has less development potential than type I and II kerogen. There are two causes for this. Firstly, type III kerogen has the least capacity to generate oil. Plankton makes up the majority of the hydrocarbon-forming organisms in type I kerogen (Peters et al., 2005), and the overall oil conversion ratio can reach 75% of the total organic carbon (Michels et al., 1995; Behar et al., 1997) (Figure 3A). The majority of type II kerogen's hydrocarbon-forming organisms are benthos (Liang et al., 2015), and their overall oil conversion ratio can surpass 35% of all organic carbon (Figure 3A). When type II kerogen reaches maturity, its total oil production is roughly 50% that of type I kerogen, and its hydrocarbon gas yield is roughly 40% that of type I kerogen (Liu S. et al., 2023; Li et al., 2024) (Figure 3B). The majority hydrocarbon-forming organisms of type-III kerogen are higher species (Chen and Peng, 2017), and relatively little oil is produced during the mature stage. Its total oil conversion ratio is less than 4.5% of total carbon. This ratio of type-III kerogen is roughly 13% of that of type II kerogen and 6% of that of type I kerogen (Farouji et al., 2023; Han et al., 2001) (Figure 3A).

Second, compared to types I and II kerogen, type III kerogen had a far lower hydrocarbon production rate. Each form of kerogen has a distinct activation energy for the production of hydrocarbons due to differences in their structures (Hou et al., 2020; Guo et al., 2024; Su et al., 2024). In type I kerogen, the aliphatic chain makes up the vast bulk. The dissociation energy of the C-C bond in both normal and isomeric alkanes is a significant chemical bond energy. The primary constituent of type III kerogen is the polycyclic aromatic structure, whose overall dissociation bond energy is significantly greater than that of C-C bonds of long-chain alkanes. The overall dissociation bond energy of type II kerogen is between that of type I and type III, as does its structure. The activation energy of hydrocarbon formation steadily increases from type I to type III kerogen, and the activation energy

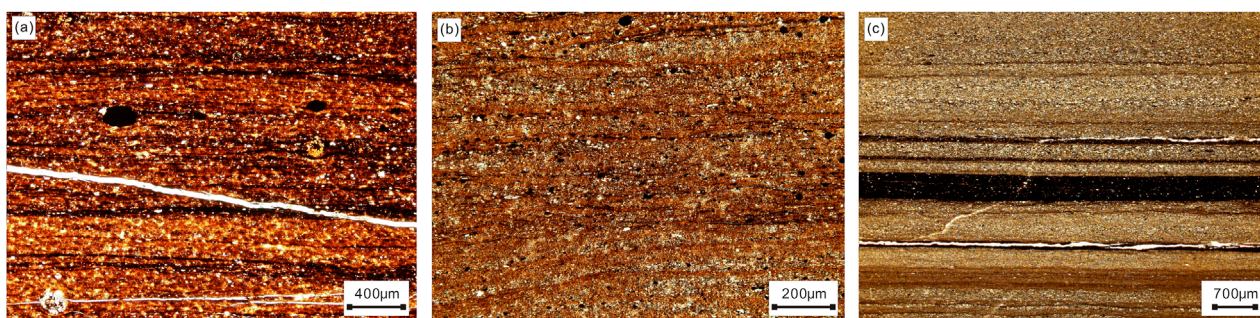


FIGURE 1 Typical microscope images of thin sections of shale facies in Chang 7 Member, the Ordos Basin. **(A)** Facies A_y shale, clear and dense lamina. **(B)** Facies B_y shale, weak deformation structure. **(C)** Facies C_y shale, flat and sparse lamina.

TABLE 1 Classification and geochemical parameters value of shale facies in the Ordos and Songliao basin.

Shale strata	Shale facies	TOC (%)	S ₁ (mg/g)	S ₂ (mg/g)	S ₁ +S ₂ (mg/g)	HI (mg/g)	Kerogen type
Chang 7 Member in the Ordos Basin (n=806)	A _y	14.6	4.82	59.11	60.72	360	II ₁
	B _y	3.8	1.89	13.38	15.59	380	II ₂
	C _y	1.4	0.59	1.94	2.53	122	III
Nenjiang Formation in the Songliao Basin (n=110)	A _n	8.1	3.34	49.87	53.21	617	I
	B _n	5.5	1.18	29.41	30.59	523	I
	C _n	3.0	1.06	15.51	16.57	505	I

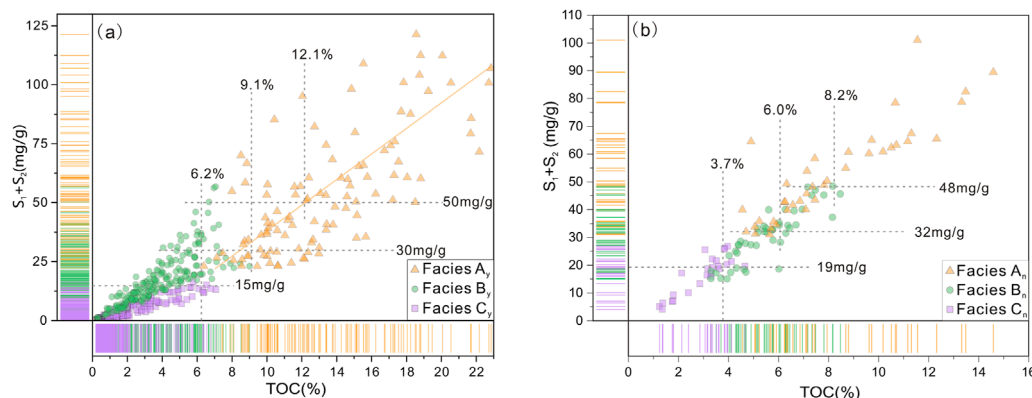


FIGURE 2 Plot of S₁+S₂ versus TOC for the shale facies in Chang 7 Member, the Ordos Basin **(A)** and in Nenjiang Formation, the Songliao Basin **(B)**.

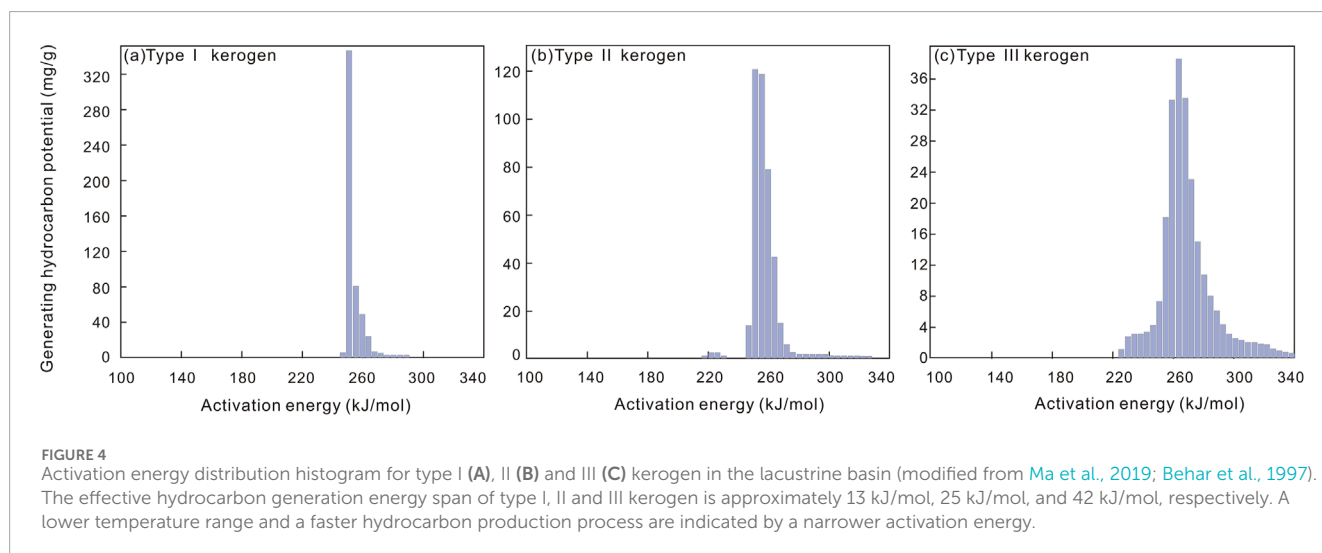
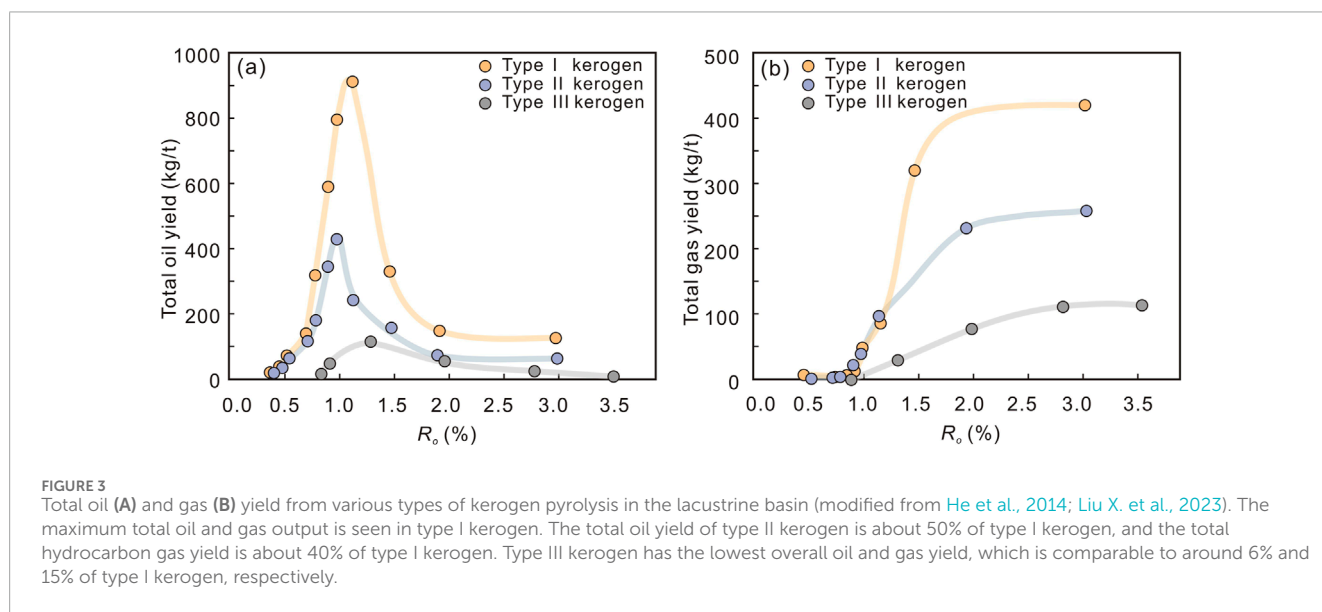
distribution gradually shifts from narrow to wide range and from asymmetric type to normal distribution (Figure 4). As a result, the type I kerogen has the ability to quickly break the chain once it reaches the primary stage of hydrocarbon formation. The effective hydrocarbon generation energy span is the narrowest (Figure 4A), indicating a quick hydrocarbon generation process in a restricted temperature range. The fraction of hydrocarbon generation between main and secondary frequency reached 80.9%. In the case of type

III kerogen, the effective hydrocarbon generation energy span is the largest (Figure 4C) and the fraction of primary and secondary frequency hydrocarbon generation is only 30.5%, indicating a very slow hydrocarbon generation process and a protracted hydrocarbon generation period. The type III kerogen has the slowest rate of hydrocarbon production. The hydrocarbon generation process of type II kerogen is slower than that of type I kerogen, but faster than that of type III kerogen, as shown in Figure 4B.

TABLE 2 Grading boundary value for the *in-situ* conversion shale oil resources in the Ordos and Songliao basin.

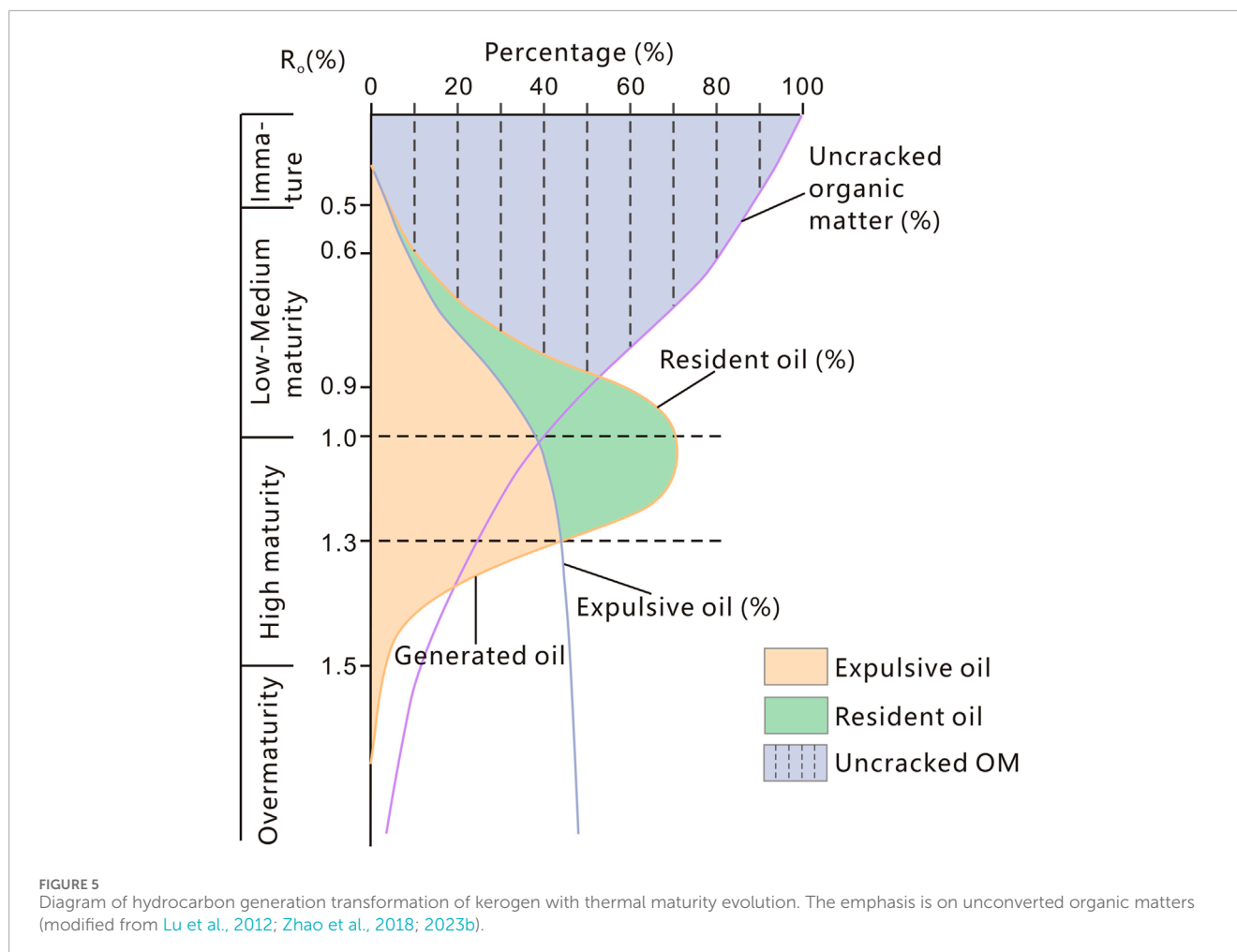
Basin	Shale strata	TOC (%)			S ₁ + S ₂ (mg/g)		
		Boundary 1st	Boundary 2nd	Boundary 3rd	Boundary 1st	Boundary 2nd	Boundary 3rd
Ordos Basin	Chang 7 Member	6.2	9.1	12.1	15	30	50
Songliao Basin	Nenjiang Formation	3.7	6.0	8.2	19	32	48

Boundary 1st: the boundary between invalid resources and valid resources; Boundary 2nd: the boundary between valid resources and sweet-spot resources; Boundary 3rd: the boundary between sweet-spot resources and core resources.



Therefore, regardless of its high TOC concentration, the shale oil production from complete thermal conversion for shale dominated by type III kerogen cannot meet the requirements for valid resource grade, making it commercially unviable for development. Only the shale dominated by types II and I kerogen is examined in

this paper. The kerogen in the shale eventually transforms into hydrocarbons with thermal evolution: 1) When $R_o < 0.6\%$, and the amount of unconverted organic matter that remains is greater than 90% (Hu et al., 2020); 2) When $R_o = 0.6\% \sim 0.9\%$, kerogen and liquid hydrocarbon that is retained coexist; 40%–90% of the kerogen is



unconverted, and the remaining liquid hydrocarbon in the shale makes up 5%–60% (Hu et al., 2020); 3) When $R_o > 1.0\%$, the amount of unconverted kerogen is less than 40% (Hu et al., 2020) (Figure 5).

Under the circumstance that the TOC content hits the lower bound for valid resources, the main constraint limiting the economic development potential of *in-situ* conversion shale oil is the thermal maturity. In situations when the R_o is less than 0.6%, most hydrocarbons have not formed spontaneously, and the *in-situ* conversion process can be utilized to maximize the yield of shale oil. The shale reaches its peak hydrocarbon generation when R_o is close to 0.9%, with at least half of the hydrocarbons not being generated. Because of the greater TOC content, *in-situ* conversion technology can still be utilized to produce a sizable amount of shale oil. When R_o is more than 1.0%, the hydrocarbon generation peak has been surpassed by the thermal evolution. Even with a reasonably high TOC, the *in-situ* conversion shale oil output falls short of the acceptable resources grade level (Figure 5).

3.3 Resource grading evaluation criteria refined by theoretical economic index

Since the empirical recoverable coefficient for *in-situ* conversion shale oil is 65%, the recovery rate in this study is fixed to a constant

value of 0.65 for comparative analysis (Guo et al., 2022; Huang et al., 2018). When heated to 330°C and held there for an extended period of time (Hou et al., 2022; Kibodeaux, 2014), the majority of the kerogen in the Chang 7 Member shale in the Ordos Basin can be converted into hydrocarbons. The heat energy needed to pyrolyze type II koregen is typically 405 MJ/t, while the rock framework has a heat capacity of 2.35 MJ/m³·°C. For instance, 23 kg of kerogen are present in 1 ton of shale. In order to fully convert the kerogen, 10.125 MJ of heat energy is needed, and 305.499 MJ are needed to raise the temperature of the rock framework from 44°C to 330°C. This results in a total energy of 315.124 MJ. Natural gas and light oil, with respective calorific values of 36 MJ/m³ and 44 MJ/kg, are the main products of the *in-situ* conversion. According to the results of a thermal simulation experiment, a ton of shale containing 23 kg of kerogen may produce about 26 m³ of natural gas and 52 kg of light oil, of which 65% are extracted. After full combustion, these hydrocarbons have a total calorific value of 2088.67 MJ. Thus, the theoretical economic index of the *in-situ* conversion shale with a TOC of 23% is approximately 6.6 (2088.67 MJ/315.124 MJ).

Because the kerogen in the Nenjiang Formation of the Songliao Basin has a lower active energy than other kerogens, most organic matter can be converted into hydrocarbons if the shales are heated to 325°C and maintained there for an extended period of time. The main products are also light oil and natural gas. The results of

TABLE 3 Calculation results of theoretical economic index*.

Basin	Shale strata	TOC (%)	Oil output (kg/t)	Gross calorific value of light oil (MJ)	Gas output (m ³ /t)	Total heat value of nature gas (MJ)	Total heat value of recoverable oil and gas (MJ)	Heat input (MJ)	Theoretical economic index /e
Ordos Basin	Chang 7 Member	6.10	16.50	726.00	7.00	249.13	633.83	307.93	2.06
		9.03	20.80	915.20	9.20	327.43	807.71	309.14	2.61
		12.10	29.50	1,298.00	10.50	373.70	1,086.60	310.36	3.50
		14.90	44.00	1936.00	17.00	605.03	1,651.67	311.57	5.30
		16.00	46.00	2024.00	20.00	711.80	1778.27	311.98	5.70
		23.10	52.00	2,288.00	26.00	925.34	2088.67	314.81	6.63
		1.60	3.75	165.00	1.25	44.49	136.17	282.65	0.48
		2.88	8.55	376.20	2.85	101.43	310.46	283.17	1.10
		2.20	5.00	220.00	1.67	59.32	181.56	282.89	0.64
		3.55	14.00	616.00	4.67	166.09	508.36	283.44	1.79
Songliao Basin	Nenjiang Formation	7.14	27.32	1,202.08	9.10	323.87	991.87	284.89	3.48
		8.10	26.90	1,183.60	8.90	316.75	975.23	285.28	3.42
		9.30	41.00	1804.00	13.60	484.02	1,487.22	285.77	5.20

*The recovery factor is set to 0.65 for the total heat values of the recoverable oil and gas. In terms of the heat input, the heating temperature for the Songliao Basin is set as 44°C–325°C, and that for the Ordos Basin is set as 44°C–330°C.

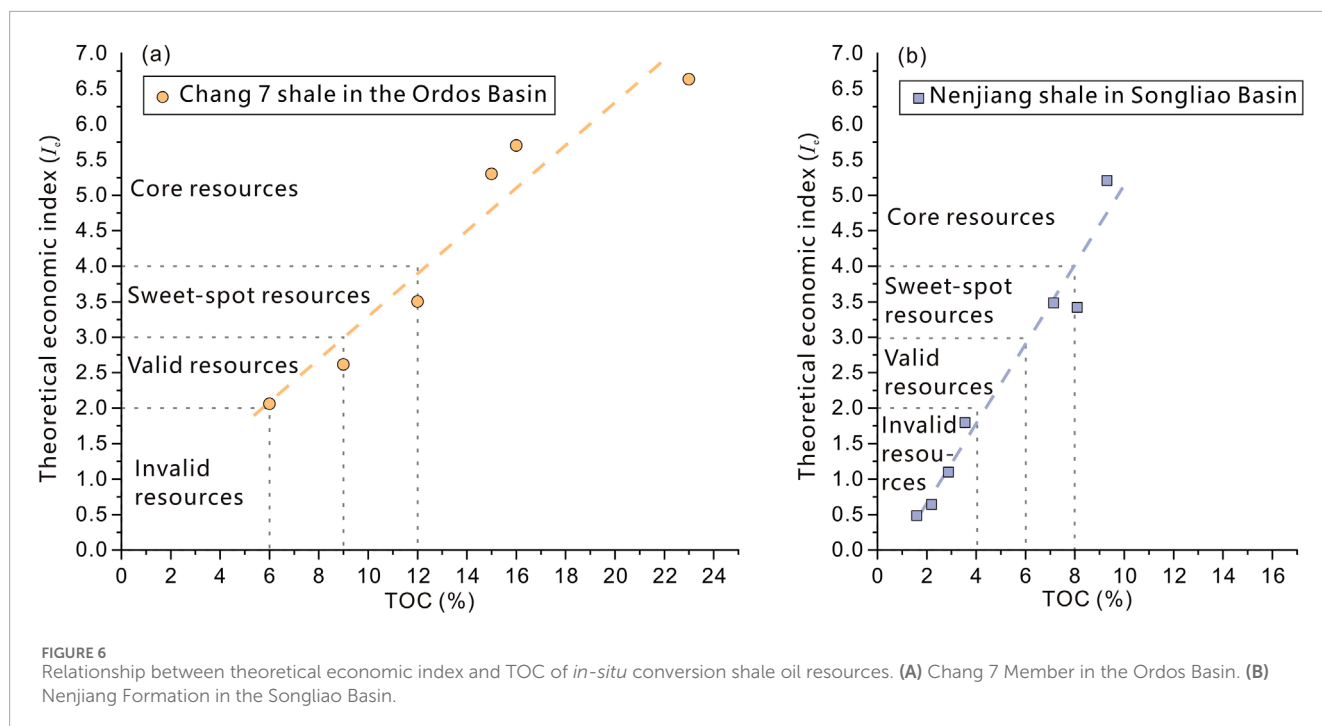


FIGURE 6 Relationship between theoretical economic index and TOC of *in-situ* conversion shale oil resources. (A) Chang 7 Member in the Ordos Basin. (B) Nenjiang Formation in the Songliao Basin.

TABLE 4 Grading evaluation criteria for *in-situ* conversion shale oil resource.

Resource grades	Chang 7 member				Nenjiang formation			
	R _o (%)	TOC (%)	S ₁ + S ₂ (mg/g)	I _e	R _o (%)	TOC (%)	S ₁ + S ₂ (mg/g)	I _e
Invalid resources	>1.0	—	—	—	>1.0	—	—	—
	≤1.0	<6	<15	<2	≤1.0	<4	<19	<2
Valid resources	≤1.0	6–9	15–30	2–3	≤1.0	4–6	19–32	2–3
Sweet-spot resources	≤0.9	9–12	30–50	3–4	≤0.9	6–8	32–48	3–4
Core resources	<0.9	≥12	≥50	>4	<0.9	≥8	>48	>4

thermal simulation experiments were used to calculate the theoretical economic indices for the two sets of shale (Table 3). As seen in Figure 6, there is a strong positive linear association between TOC and theoretical economic index (I_e) based on the experimental data and the I_e computation results of many shale samples.

Only when the theoretical economic index (I_e) satisfies the condition of being more than or equal to 2 can the development of commercially viable resources be possible, provided that the investment and operating expenses are simplified. In relation to the Chang 7 shale, the corresponding TOC needs to be precisely larger than or equal to 6% (Figure 6), which is in close proximity to the value at the first boundary (Table 2). When the theoretical economic index (I_e) is more than or equal to 3, these shales can yield shale oil resources above sweet-spot grade by *in-situ* conversion technology. The TOC corresponding to this index is 9%, which is close to the value at second boundary (Table 2). Similarly, these shales can produce shale oil resources above core grade when the theoretical economic index (I_e) is more than or equal to 4.

The TOC corresponding to this index is 12%, which is near to the value at the third boundary (Table 2). When the indices for the shales in Nenjiang Formation in the Songliao Basin are 2, 3, and 4, respectively, the corresponding TOC values are 4%, 6%, and 8% (Figure 6). These values are quite near the boundaries of the four resource grades (Table 2). As a result, we discover a strong correlation between the resource grading and the theoretical economic index. It is evident that the theoretical economic index can be used to further enhance the grading evaluation criteria for *in-situ* conversion shale oil resources. The updated resource grading evaluation criteria, which fully incorporates thermal maturity and the theoretical economic index, are displayed in Table 4. To make generalization easier, the value of TOC has been revised to an integer.

In contrast to medium-high maturity shale oil, the approach used in this study solely takes the mass of the rock into account, ignoring its thickness. It is important to note that organic-rich shale in medium-low maturity can be converted into valuable resources regardless of thickness based on the principles of *in-situ*

TABLE 5 Area and amount of graded *in-situ* conversion shale oil resources in the Chang7 Member, the Ordos Basin.

Resource grade	Location (see Figure 7)	Prospective area (km ²)	Risked recoverable Resource (10 ^{×6} ton)
Core resources	C1	1,251.03	34,522.52
	C2	121.55	2,892.03
	C3	530.91	4,492.51
	C4	10,000.19	92,696.29
	Sum of core resources	11,903.68	134,603.35
Sweet-spot resources	SP1	1,198.28	20,557.96
	SP2	7,305.50	74,076.60
	Sum of sweet-spot resources	8,503.78	94,634.56
Valid resources	V1	1764.74	13,569.10
	V2	8,463.64	102,295.25
	V3	107.79	541.91
	Sum of valid resources	10,336.17	116,406.25
Invalid resources	IV1	378.40	3,959.52
	IV2	1,669.57	15,980.69
	IV3	3,860.87	34,776.06
	Sum of invalid resources	5,908.84	54,716.28
Total		36,652.47	400,360.44

conversion technology. An increase in thickness may result in a proportional rise in energy usage. However, very thin shale can cause development challenges or not be economically feasible given the state of technology currently. Thus, based on a variety of field test results (Sun et al., 2021), it is advised to set the lower limit for the thickness of *in-situ* conversion shale at 5 m.

4 Application of grading evaluation criteria

Based on core sampling, well logging data and isoline maps, in this study, we graded the *in-situ* conversion shale oil resources of the Chang 7 Member. By overlaying the TOC isoline map, vitrinite reflectance (R_o) isogram, shale isopach map and hydrocarbon generation potential (S_1+S_2) isoline map, according to the grading evaluation criteria described above, the area that is rich in *in-situ* conversion shale oil resources can be delineated.

The first step was delineating the areas where the shale thickness is greater than or equal to 5 m, and then, the areas with $R_o \leq 1.0\%$ and $R_o \leq 0.9\%$ were delineated. Then the area that meets the criteria $R_o \leq 0.9\%$, $TOC \geq 12\%$, and $S_1+S_2 \geq 50$ mg/g was classified as core resources; the area meets the criteria $R_o \leq 0.9\%$, $12\% \geq TOC \geq 9\%$, and 50 mg/g $\geq S_1+S_2 \geq 30$ mg/g was classified as sweet-spot

resources; the area that meets the criteria $R_o \leq 0.9\%$, $9\% \geq TOC \geq 6\%$, and 30 mg/g $\geq S_1+S_2 \geq 15$ mg/g was classified as valid resources; and the that meets the criteria that $R_o > 1.0\%$, $TOC < 6\%$, and $S_1+S_2 < 15$ mg/g was classified as invalid resources. The areas and amount of the four grades of resources are summarized in Table 5.

For the Chang 7 Member in the Ordos Basin, the shale is distributed widely and continuously, and the thermal maturity is generally low. The area containing core resources of *in-situ* conversion shale oil is mainly located in the Jiyuan area (C1 in Figure 7), eastern part of the Yanwu area (C2 and C3 in Figure 7), and southern part of the basin (C4 in Figure 7), with a risked recoverable resource of 13.46 billion tons (Table 5). The area containing sweet-spot resources (8,503 km²) is mainly located in Jiyuan area (SP1 in Figure 7), Huanxian-Qingyang-Zhengning area (SP2 in Figure 7), with a risked recoverable resource of 9.46 billion tons (Table 5). The area containing valid resources is 10,336 km² and is broadly distributed in areas such as Majiapu-Dingbian (V1 in Figure 7) and Gengwan-Huachi-Yijun (V2 in Figure 7), with a risked recoverable resource of 11.64 billion tons (Table 5). In addition, the area containing invalid resources is concentrated in the regions with high maturity, including the western Dingbian area (IV1 in Figure 7), Gengwan-Baibao area (IV2 in Figure 7), and Chenghao-Nanliang-Ta'erwan area (IV3 in Figure 7), with an area of approximately 5,909 km² (Table 5).

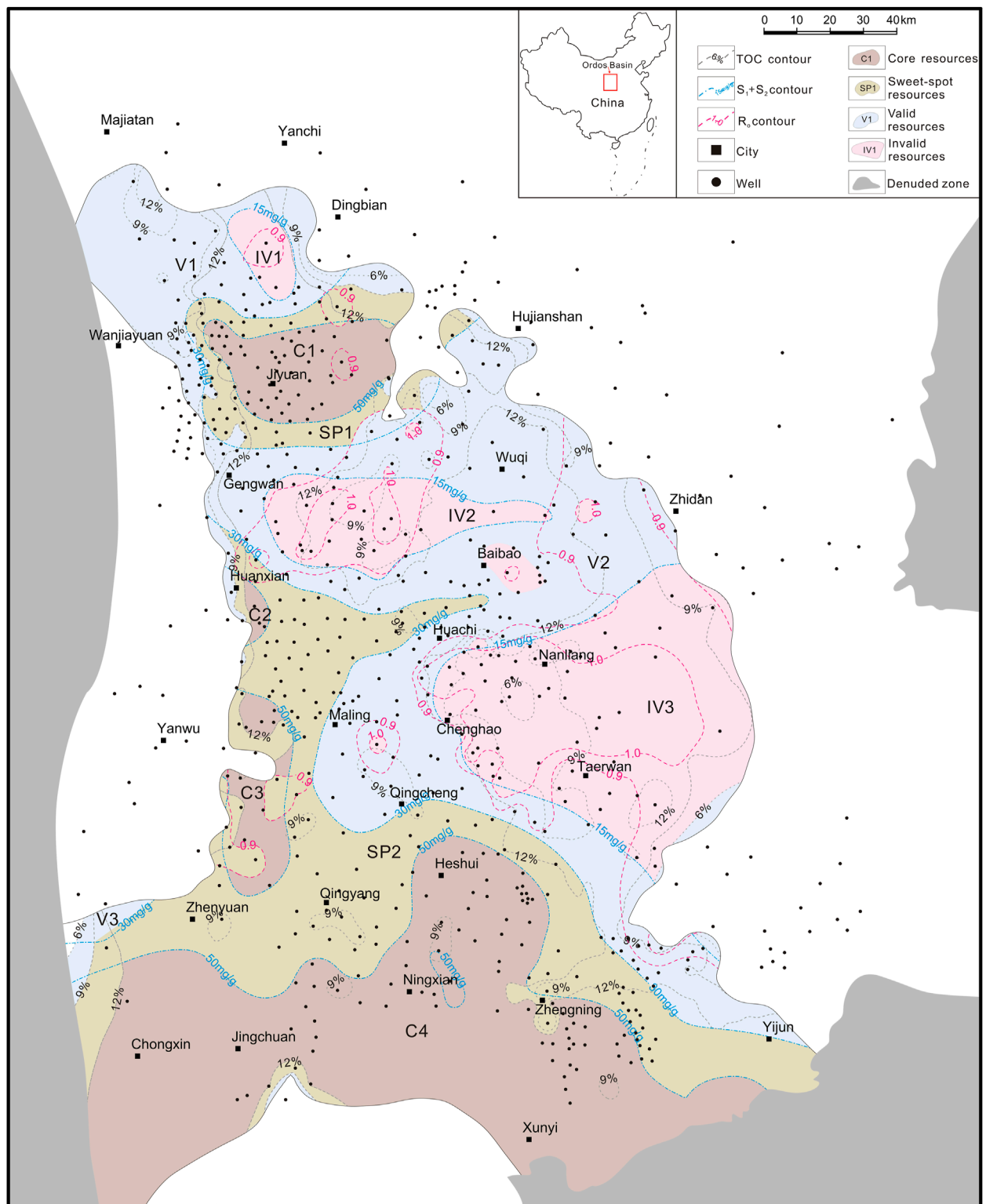


FIGURE 7
 Composite evaluation map of *in-situ* conversion shale oil resource in Chang7 Member, the Ordos Basin. There are four core resource areas (orange color, C1, C2, C3 and C4), with the largest core resource located in the southern part of the basin. There are mainly two sweet-spot resource areas (yellow color, SP1 and SP2), SP2 occupies most of the sweet-spot resources and is located in the west and eastern part of the basin. With SP1 as the boundary, the valid resource area (green color) is mainly composed of the northern part (V1) and the central-eastern part (V2) of the basin. Three major (gray color, V1, V2, and V3) and a few sporadic invalid resource areas are located within the valid resource area.

This initial assessment shows how the various resource grades are distributed. However, more investigation is required to ascertain which area is best suited for development; which area has an excessive burial depth that might make drilling more expensive and challenging; which area has naturally occurring fractures that might result in heat loss during heating; and which area might contain active water that might result in a large rise in energy consumption.

5 Conclusion

Based on the statistical analysis of petrological and geochemical data, we conclude as follows:

- (1) Shale's facies classification is a crucial factor in resource grading assessments. Using the lacustrine shale of the Chang 7 Member in the Ordos Basin and the Nenjiang Formation in the Songliao Basin as examples, facies C shale represents the invalid resources and facies B shale represents the valid resources. Furthermore, the portion of facies A shale with a relatively low potential for producing hydrocarbons is represented by the sweet-spot resources, whilst the portion with a relatively high potential for producing hydrocarbons is represented by the core resources.
- (2) The theoretical economic index (I_e) represents the energy input-output ratio of shale oil production by *in-situ* conversion technology, and can be used as an important parameter for resource grading evaluation. $I_e = 2$ is the lower limit of valid resources for *in-situ* conversion shale oil. $I_e = 3$ is the lower limit of sweet-spot resources and $I_e = 4$ is the lower limit of core resources.
- (3) Although the invalid resource represents an inefficient energy replacement from the perspective of energy input and output, these shale oil resources may still be economical to exploit under the conditions of increasingly cheap renewable energy supply (such as wind and photovoltaic power). Considering oil and gas as a strategic energy source, it is necessary to explore and develop the invalid resource of *in-situ* conversion shale oil as a prospective petroleum resource in future.
- (4) Thermal simulation experiments in the laboratory cannot completely restore the actual underground heating process, especially the nonlinearity and heterogeneity of heat conduction. Therefore, the thermochemical result parameters may be biased. The calculation of the theoretical economic index (I_e) only considers the input of energy consumption and the total calorific value of the products, which is obviously oversimplified. In order to obtain a more accurate evaluation, it may be necessary in the future to include more indicators—such as the anisotropy of thermal conductivity, energy loss of various heating models, total heating time, etc.—into the theoretical economic index (I_e) calculation and resource evaluation system.

Data availability statement

The datasets used and/or analysed during the current study available from the corresponding author on reasonable request.

Author contributions

SeL: Conceptualization, Methodology, Writing—original draft, Writing—review and editing. XL: Project administration, Writing—original draft. ZZ: Investigation, Resources, Writing—review and editing. LH: Investigation, Writing—original draft. ShL: Formal Analysis, Investigation, Writing—review and editing. HL: Resources, Validation, Writing—review and editing. ZP: Investigation, Writing—review and editing. LZ: Formal Analysis, Writing—review and editing.

Funding

The author(s) declare that financial support was received for the research, authorship, and/or publication of this article. This research is supported by China National Petroleum Corporation Scientific research and technology development project [No. 2021DJ5202]. The funder was not involved in the study design, collection, analysis, interpretation of data, the writing of this article, or the decision to submit it for publication.

Acknowledgments

The authors sincerely appreciate the financial support from the China National Petroleum Corporation. The authors would like to thank the Editor, the Associate Editor, and the reviewers for their constructive comments that improved this paper.

Conflict of interest

Authors SeL, XL, ZZ, LH, ZP, and LZ were employed by PetroChina. Author ShL was employed by CNPC Shenzhen New Energy Research Institute Co., Ltd.

The remaining author declares that the research was conducted in the absence of any commercial or financial relationships that could be construed as a potential conflict of interest.

Generative AI statement

The author(s) declare that no Generative AI was used in the creation of this manuscript.

Publisher's note

All claims expressed in this article are solely those of the authors and do not necessarily represent those of their affiliated organizations, or those of the publisher, the editors and the reviewers. Any product that may be evaluated in this article, or claim that may be made by its manufacturer, is not guaranteed or endorsed by the publisher.

References

- Alpak, F. O., Vink, J. C., Gao, G., and Mo, W. (2013). Techniques for effective simulation, optimization, and uncertainty quantification of the *in-situ* upgrading process. *J. Unconv. Oil and Gas Resour.* 3-4 (S3/S4), 1–14. doi:10.1016/j.juogr.2013.09.001
- Arrhenius, S. (1889). Über die Reaktionsgeschwindigkeit bei der Inversion von Rohrzucker durch Säuren. *Z. für Phys. Chem.* 4 (1), 226–248. doi:10.1515/zpch-1889-0416
- Behar, H., Vandenbroucke, M., Tang, Y., Marquis, F., and Espitalie, J. (1997). Thermal cracking of kerogen in open and closed systems: determination of kinetic parameters and stoichiometric coefficients for oil and gas generation. *Org. Geochem.* 26, 321–339. doi:10.1016/S0146-6380(97)00014-4
- Chen, J., and Peng, P. (2017). A comparative study of free and bound bitumens from different mature source rocks with Type III kerogens. *Org. Geochem.* 112, 1–15. doi:10.1016/j.orggeochem.2017.06.014
- Connan, J. (1974). Time-temperature relation in oil genesis: geologic notes. *AAPG Bull.* 58 (12), 2516–2521. doi:10.1306/83D91BEB-16C7-11D7-8645000102C1865D
- Cui, J., Zhu, R., Hou, L., Wu, S., Mao, Z., and Li, S. (2018). Shale *in-situ* mining technology *status quo* of challenges and opportunities. *Unconv. Oil and Gas* 5 (6), 103–114. doi:10.3969/j.issn.2095-8471.2018.06.017
- Deng, M., Duan, X., Zhai, C., Long, S., Yang, Z., Deng, L., et al. (2020). Variation in liquid hydrocarbon content during thermal simulation and its influence on physical property of shale. *Oil and Gas Geol.* 41 (6), 1310–1320. doi:10.11743/ogg20200619
- Dyni, J. R. (2003). Geology and resources of some world oil-shale deposits. *Oil Shale* 20 (3), 193–252. doi:10.3176/oil.2003.3.02
- EIA (2013). *Technically recoverable shale oil and shale gas resources: an assessment of 137 shale formations in 41 countries outside the United States*. Washington.
- Farouji, M. S., Liu, B., Gentzis, T., Wen, Z., Ma, Z., Bai, L., et al. (2023). Geochemical evolution of kerogen type III during hydrous pyrolysis: a case study from the Damoguaihe Formation, Hailar Basin, China. *Geoenergy Sci. Eng.* 228, 211947. doi:10.1016/j.geoen.2023.211947
- Guo, C., Li, M., Liu, X., Xiao, H., Luo, Q., Han, Q., et al. (2024). Construction of multidimensional structure model of the Mesoproterozoic Xiamaling shale kerogen, northern North China. *Fuel* 367, 131572. doi:10.1016/j.fuel.2024.131572
- Guo, Q., Chen, X., Liuzhuang, X., Yang, Z., Zheng, M., Chen, N., et al. (2020). Evaluation method for resource potential of shale oil in the triassic yanhang Formation of the Ordos Basin, China. *Energy Explor. and Exploitation* 38 (4), 841–866. doi:10.1177/0144598720903394
- Guo, Q., Hou, L., Wang, J., Liuzhuang, X., Luo, X., and Chen, N. (2022). An evaluation method of resource potential of *in-situ* converted shale oil and its application. *Acta Pet. Sin.* 43 (12), 1750–1757. doi:10.7623/syxb202212006
- Guo, Q., Mi, Y., Zhang, Q., and Wang, J. (2023). Assessment methods and potential of shale oil resources in China. *Petroleum Geol. and Exp.* 45 (3), 402–412. doi:10.11781/sydz202303402
- Han, Z., Yang, Q., and Pang, Z. (2001). Artificial maturation study of a humic coal and a torbanite. *Int. J. Coal Geol.* 46, 133–143. doi:10.1016/S0166-5162(01)00018-0
- He, K., Zhang, S., Wang, X., Mi, J., and Mao, R. (2014). Hydrocarbon generation kinetics of type-I organic matters in the Cretaceous lacustrine sequences, Songliao Basin. *Oil Gas Geol.* 35 (1), 42–49. doi:10.11743/ogg20140106
- Hou, L., He, K., Zhai, J., Mi, J., and Weng, N. (2022). Compositional kinetics for hydrocarbon evolution in the pyrolysis of the Chang 7 organic matter: implications for *in-situ* conversion of oil shale. *J. Anal. Appl. Pyrolysis* 162, 105434. doi:10.1016/j.jaap.2022.105434
- Hou, L., Ma, W., Luo, X., Tao, S., Guan, P., and Liu, J. (2020). Chemical structure changes of lacustrine Type-II kerogen under semi-open pyrolysis as investigated by solid-state ¹³C NMR and FT-IR spectroscopy. *Mar. Petroleum Geol.* 116, 104348. doi:10.1016/j.marpetgeo.2020.104348
- Hu, S., Zhao, W., Hou, L., Yang, Z., Zhu, R., Wu, S., et al. (2020). Development potential and technical strategy of continental shale oil in China. *Petroleum Explor. Dev.* 47 (4), 877–887. doi:10.1016/S1876-3804(20)60103-3
- Huang, Z., Liu, Q., Li, M., Chen, J., Li, P., and Zhang, R. (2018). Hydrocarbon expulsion efficiency and oil-bearing property of the shale system in Chang 7 Member, Ordos Basin. *Oil and Gas Geol.* 39 (3), 513–521 + 600. doi:10.11743/ogg20180308
- Jin, Z., Bai, Z., Gao, B., and Li, M. (2019). Has China ushered in the shale oil and gas revolution? *Oil Gas Geol.* 40 (3), 451–458. doi:10.11743/ogg20190301
- Kang, Z., Zhao, Y., and Yang, D. (2020). Review of oil shale *in-situ* conversion technology. *Appl. Energy* 269, 115121. doi:10.1016/j.apenergy.2020.115121
- Kibodeaux, K. R. (2014). Evolution of porosity, permeability, and fluid saturations during thermal conversion of oil shale. *SPE 170733-MS*. doi:10.2118/170733-MS
- Li, C., Jin, Z., Zhang, L., and Liang, X. (2024). Thermodynamic and microstructural properties of the lacustrine Chang-7 shale kerogen: implications for *in-situ* conversion of shale. *Int. J. Coal Geol.* 283, 104447. doi:10.1016/j.coal.2024.104447
- Liang, M., Wang, Z., Zheng, J., Li, X., Wang, X., Gao, Z., et al. (2015). Hydrous pyrolysis of different kerogen types of source rock at high temperature - bulk results and biomarkers. *J. Petroleum Sci. Eng.* 125, 209–217. doi:10.1016/j.petrol.2014.11.021
- Lin, S., Yang, Z., Hou, L., Luo, X., and Liu, Q. (2019). Geostatistical recognition of genetically distinct shale facies in upper Triassic Chang 7 section, the Ordos Basin, North China. *Mar. Petroleum Geol.* 102, 176–186. doi:10.1016/j.marpetgeo.2018.11.050
- Liu, S., Gao, G., Jin, J., Zhang, L., Gang, W., Xiang, B., et al. (2023). Significance of hydrocarbon generation characteristics of source rock samples dominated by telalginite and lamalginite in saline lacustrine sediments. *Acta Geol. Sin.* 97 (3), 879–887. doi:10.19762/j.cnki.dizhixuebao.2022015
- Liu, X., Wang, Q., Jia, W., Song, J., and Peng, P. (2023). Pyrolysis of an organic-rich shale containing type II kerogen before and after oil generation and expulsion: implications for the generation of late hydrocarbon and hydrogen gases. *J. Anal. Appl. Pyrolysis* 173, 106105. doi:10.1016/j.jaap.2023.106105
- Liu, Z., Dong, Q., Ye, S., Zhu, J., Guo, W., Li, D., et al. (2006). The situation of oil shale resources in China. *J. Jilin Univ. (Earth Sci Ed)* 36, 869–876. doi:10.3969/j.issn.1671-5888.2006.06.002
- Liu, Z., Meng, Q., Dong, Q., Zhu, J., Guo, W., Ye, S., et al. (2017). Characteristics and resource potential of oil shale in China. *Oil Shale* 34, 15–41. doi:10.3176/oil.2017.1.02
- Lu, S., Huang, W., Chen, F., Li, J., Wang, M., Xue, H., et al. (2012). Classification and evaluation criteria of shale oil and gas resources: discussion and application. *Petroleum Explor. Dev.* 39 (2), 268–276. doi:10.1016/S1876-3804(12)60042-1
- Ma, X., Li, M., Jiang, Q., Qian, M., Li, Z., and Pang, X. (2019). Chemical kinetic model for quantitative evaluation on oil-bearing property of lacustrine shale. *Petroleum Geol. Recovery Effic.* 26 (1), 137–151. doi:10.13673/j.cnki.cn37-1359/te.2019.01.015
- Michels, R., Landais, P., Torkelson, B. E., and Philip, R. P. (1995). Effects of effluents and water pressure on oil generation during confined pyrolysis and high-pressure hydrous pyrolysis. *Geochimica Cosmochimica Acta* 59, 1589–1604. doi:10.1016/0016-7037(95)00065-8
- Pang, X., and Chen, Z. (1997). Basic concept of hydrocarbon expulsion threshold and its research significance and application. *Geoscience* 11 (4), 510–521.
- Peters, K. E., Walters, C. C., and Moldowan, J. M. (2005). *The biomarker guide: interpreting molecular fossils in petroleum and ancient sediments*. second edn. UK: Cambridge University Press.
- Su, C., Liu, Y., Yang, Y., Gao, T., Qi, T., and Wang, Y. (2024). Evolution of aromatic structure and nanopores in shale kerogen by using *in-situ* HRTEM and *in-situ* FT-IR experiment. *Fuel* 359, 130479. doi:10.1016/j.fuel.2023.130479
- Sun, Y., Guo, W., and Deng, S. (2021). The status and development trend of *in-situ* conversion and drilling exploitation technology for oil shale. *Drill. Eng.* 48 (1), 57–67. doi:10.12143/j.ztgc.2021.01.008
- Sun, Y., Guo, W., Li, Q., Bai, F., and Deng, S. (2023). Current status and prospects of oil shale *in-situ* conversion technology in China. *Petroleum Sci. Bull.* 4, 475–490. doi:10.3969/j.issn.2096-1693.2023.04.036
- Wang, Y., Wang, Y., Meng, X., Su, J., Li, F., and Li, Z. (2013). Enlightenment of American's oil shale *in-situ* retorting technology. *Oil Drill. and Prod. Technol.* 35 (6), 55–59.
- Yu, Y., Wang, H., Liu, D., Zhao, Q., Li, X., Wu, J., et al. (2023). Development status and feasibility evaluation index system of continental shale oil demonstration area in China. *Earth Sci.* 48 (1), 191–205. doi:10.3799/dqkx.2022.422
- Zhang, D., Huang, D., Li, J., and Zhang, Y. (1983). Kinetic features of thermo-degradation of kerogens in oil shales and their geochemical significances. *Oil and Gas Geol.* 4 (4), 383–393.
- Zhao, W., Bian, C., Li, Y., Liu, W., Dong, J., Wang, K., et al. (2023b). Organic matter transformation ratio, hydrocarbon expulsion efficiency and shale oil enrichment type in Chang 7₃ shale of Upper Triassic Yanhang Formation in Ordos Basin, NW China. *Petroleum Explor. Dev.* 50 (1), 14–26. doi:10.1016/S1876-3804(22)60366-5
- Zhao, W., Hu, S., and Hou, L. (2018). Connotation and strategic role of *in-situ* conversion processing of shale oil underground in the onshore China. *Petroleum Explor. Dev.* 45 (4), 563–572. doi:10.1016/S1876-3804(18)30063-6
- Zhao, W., Hu, S., Hou, L., Yang, T., Li, X., Guo, B., et al. (2020). Types and resource potential of continental shale oil in China and its boundary with tight oil. *Pet. Explor. Dev.* 47 (1), 1–11. doi:10.1016/S1876-3804(20)60001-5
- Zhao, W., Zhao, Y., Li, G., Hu, S., Zhu, R., Bian, C., et al. (2023a). Scientific problems and key technologies of enrichment and *in-situ* transformation of mid-low mature shale oil in continental facies. *Sci. Found. China* 37 (2), 276–284.